JACS
JOURNAL OF THE AMERICAN CHEMICAL SOCIETY
Communication
pubs.acs.org/JACS

Site-Dependent Activity of Atomic Ti Catalysts in Al-Based Hydrogen Storage Materials

Abdullah Al-Mahboob,[†] Erik Muller,[†] Altaf Karim,[‡] James T. Muckerman,[‡] Cristian V. Ciobanu,[§] and Peter Sutter*[,†]

[†]Center for Functional Nanomaterials, Brookhaven National Laboratory, Upton, New York 11973, United States

[‡]Department of Chemistry, Brookhaven National Laboratory, Upton, New York 11973, United States

[§]Department of Mechanical Engineering, Materials Science Program, Colorado School of Mines, Golden, Colorado 80401, United States

Supporting Information

ABSTRACT: Doping catalytically inactive materials with dispersed atoms of an active species is a promising route toward realizing ultradilute binary catalyst systems. Beyond catalysis, strategically placed metal atoms can accelerate a wide range of solid-state reactions, particularly in hydrogen storage processes. Here we analyze the role of atomic Ti catalysts in the hydrogenation of Al-based hydrogen storage materials. We show that Ti atoms near the Al surface activate gas-phase H_2, a key step toward hydrogenation. By controlling the placement of Ti, we have found that the overall reaction, comprising H_2 dissociation and H spillover onto the Al surface, is governed by a pronounced trade-off between lowering of the H_2 dissociation barrier and trapping of the products near the active site, with a sharp maximum in the overall activity for Ti in the subsurface layer. Our findings demonstrate the importance of controlling the placement of the active species in optimizing the activity of dilute binary systems.

An important recent thrust in heterogeneous nanocatalysis has been motivated by the need to minimize the use of noble metals (Pt, Pd, Rh), which has been done, for example, by designing bimetallic alloys[1] or core–shell structures.[1,2] Calculations[3−5] and experiments[6] have suggested that such engineered structures may offer new degrees of freedom (coordination, strain) whose optimization (via predictable d-band center shifts[7,8]) may give rise to activity exceeding that of the noble metal. Particularly interesting but probably least explored is the dilute limit, wherein individual atoms of an active species embedded in an inactive matrix catalyze a reaction and transfer the products onto the matrix for further conversion. Here, the catalyst and matrix as well the placement of the active species become factors controlling the activity, as suggested by recent studies of Pd:Cu and Pd:Au bimetallic surfaces, which showed H_2 dissociation by Pd:Cu(111)[9] but not by Pd:Au(111).[10]

Emerging applications in heterogeneous catalysis indicate that dilute atomic catalysts may also be useful in other contexts. An important example involves hydrogenation reactions in solid-state hydrogen storage, an enabling technology for fuel handling in a renewable-energy-based economy.[11,12] High interest in transition-metal-doped complex hydrides was initially stimulated by work on $NaAlH_4$ by Bogdanovic and Schwickardi[13] showing that Ti dopants can significantly improve the hydrogen uptake/release kinetics. While doping in this system affects multiple properties, such as the bulk defect chemistry,[14−16] there is strong evidence that key reaction steps promoted by dopants occur at the solid–gas interface,[17−19] catalytic H_2 activation being one of the primary roles of Ti.[20,21] More recently, aluminum hydride (AlH_3) has attracted interest as a promising high-capacity (10 wt %) Al-based hydrogen storage material, but its large-scale application has been hindered by the lack of a facile regeneration pathway. Several solvent-based hydrogenation routes using stabilization as amine alane[22,23] or polar solvent adducts[24] have been demonstrated. The common feature of these approaches is the use of Ti-catalyzed ("activated") Al* powders as a starting material for hydrogenation.

Here we establish the interaction of H_2 with Ti-catalyzed Al, which is relevant to the hydrogenation of AlH_3, $NaAlH_4$, and other Al-based materials, by considering a Ti:Al(111) model system using scanning tunneling microscopy (STM) and density functional theory (DFT). The focus is on the initial steps of hydrogenation: H_2 dissociation and spillover of H onto the Al surface. A particular response of stepped Al(111) to atomic hydrogen, H-induced Ostwald ripening, was used to detect the presence of H originating from the catalytic dissociation of H_2. Details of this process will be discussed in a separate publication. The basic phenomenon is shown in Figure 1. While stepped Al(111) with excess monolayer (ML) islands and pits is stable at 300 K, the exposure to atomic H triggers the rapid onset of ripening (i.e., decay of Al islands and concurrent filling of pits).[25] Calculations show that the island decay involves formation of Al hydrides at steps and their detachment and diffusion on the Al(111) terraces. Dissociation of Al hydride liberates Al monomers that can reattach to Al steps. The curvature-dependent chemical potential drives the simultaneous net decay of Al(111) islands and vacancy islands (Figure 1 f).

To detect H_2 dissociation and H spillover, we performed real-time STM observations during exposure to H_2 gas on

Received: May 1, 2012
Published: June 13, 2012

   dx.doi.org/10.1021/ja304203y | J. Am. Chem. Soc. 2012, 134, 10381−10384

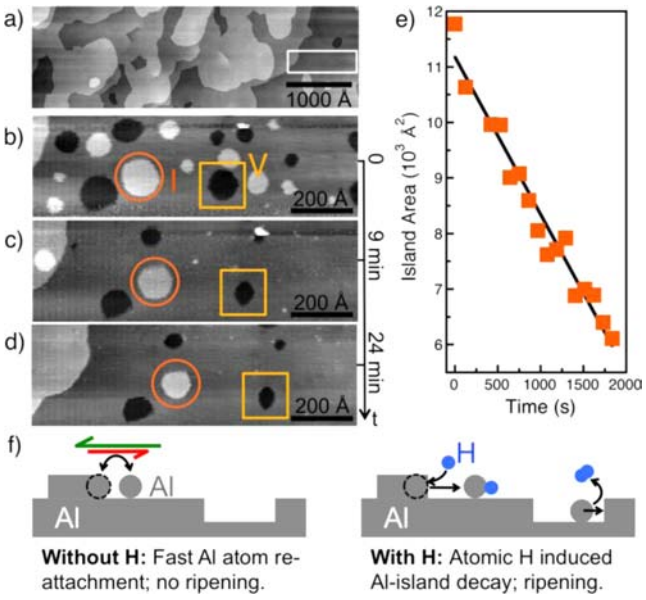

Figure 1. Decay of Al islands and pits upon exposure to atomic hydrogen. (a) STM image of clean Al(111). (b) Monolayer (ML)-high Al islands (I) and ML-deep pits (vacancy islands, V) were formed by tip manipulation within the rectangle in (a). (b–d) Time-lapse STM (at 300 K) before and during H dosing. H was generated by a cracker (45 W, $P_{H_2} = 5 \times 10^{-9}$ Torr). (e) Areal decay of one Al island (marked in b–d) under atomic H. The line is a linear fit of the island area, $A(t)$. (f) Inefficient step detachment for Al(111) due to a low reattachment barrier (left) and facile step detachment and Ostwald ripening induced by atomic H (right).

samples in which the location of the Ti dopants was changed systematically: (i) Ti adatoms; (ii) Ti atoms embedded in the Al surface; and (iii) Ti atoms in the subsurface layer [methods are described in the Supporting Information (SI)]. Exposure of Al(111) without Ti to H_2 showed no H-induced ripening, consistent with the absence of atomic H due to the high (>1 eV) activation energy for H_2 dissociation on Al(111) (Figures S1 and S2 in the SI). Two types of Ti-doped samples, one prepared with Ti adatoms (ad-Ti) and the other with substitutional Ti embedded in the Al(111) surface, also showed no H-induced ripening and thus either do not dissociate H_2 or preclude the spillover of H away from the Ti sites. STM and DFT calculations (discussed below) suggest that Ti atoms in both types of sites indeed catalyze H_2 dissociation but that the products remain strongly bound near the catalyst (see Figure 2 for Ti alloyed into the top Al layer). At 300 K, Ti/Al(111) is kinetically stabilized in the surface layer, where it is incorporated by quasi-random replacement of Al atoms and is imaged as shallow protrusions in STM.[19] Imaging during H_2 exposure indeed showed this appearance of Ti atoms but also transient contrast changes that DFT-based STM simulations showed to be due to binding of H atoms in specific sites near Ti. These observations are consistent with H_2 dissociation by Ti, with the resulting H atoms becoming trapped near the Ti sites for a long enough time to be imaged by STM. Extensive STM observations of ad-Ti and substitutional surface Ti at H_2 pressures up to 5×10^{-5} Torr showed no onset of H-induced Ostwald ripening, supporting the conclusion that H spillover was suppressed.

H_2 activation and H spillover may be enabled simultaneously by weakening the binding of H to the catalyst via Ti placement in subsurface layers. Subsurface Ti can be obtained via annealing of dilute Al:Ti surface alloys.[19,26] Here, we instead covered mixed Al:Ti surfaces (1–2 ML; < 10 atom % Ti) with a skin of pure Al (1.3 ML, to generate an ML island/pit morphology). Subsurface Ti was confirmed by a characteristic inverted STM contrast.[19] The effect of exposing Al(111) with subsurface Ti to H_2 was studied by time-lapse STM (Figure 3), which clearly showed the onset of Al(111) island/pit decay, that is, the characteristic H-induced Ostwald ripening demonstrating the generation of atomic H. We conclude that subsurface Ti atoms are able to catalyze H_2 dissociation and that their interaction with the products is sufficiently weak to allow spillover of H to Al surface sites.

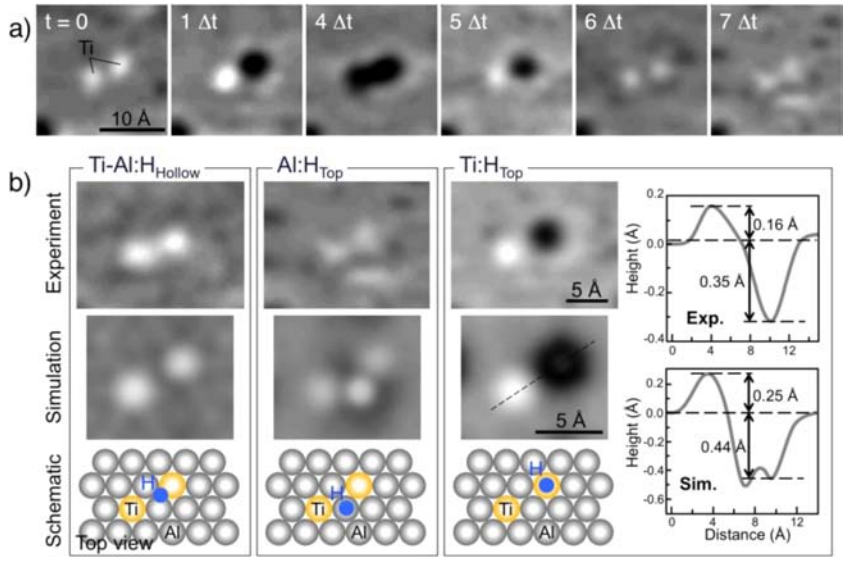

Figure 2. H_2 dissociation and H trapping near Ti embedded in the Al(111) surface. (a) Time-lapse STM in the vicinity of two Ti atoms in the Al(111) surface[19] during exposure to 10^{-5} Torr H_2 ($\Delta t \approx 10$ s; $U = +1.8$ V; $I = 0.2$ nA; $T = 300$ K). (b) Comparison of experimental STM images with DFT-based STM simulations for three configurations of H atoms bound near a Ti atom pair and experimental and simulated height profiles for the Ti:H_{top} configuration.

dx.doi.org/10.1021/ja304203y | J. Am. Chem. Soc. 2012, 134, 10381–10384

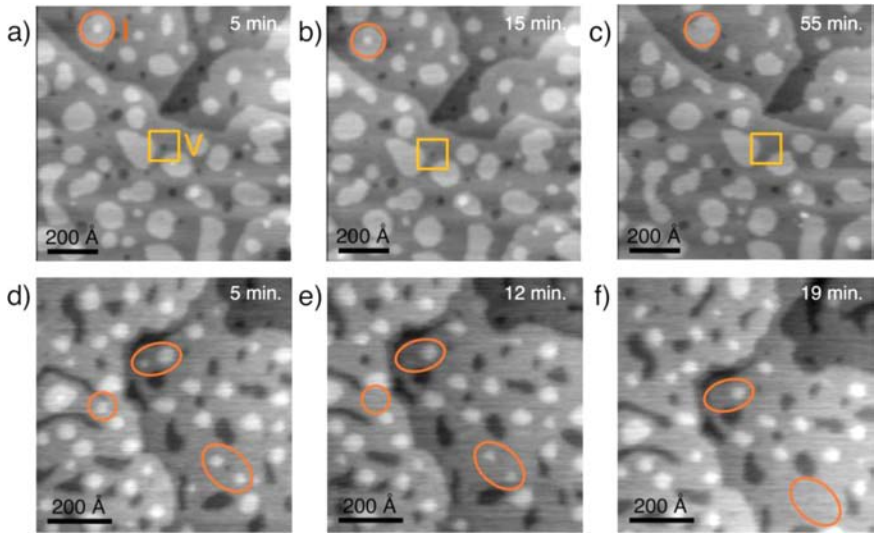

Figure 3. H_2 dissociation by Ti in the subsurface Al layer and spillover of H onto Al(111). (a–c) Time-lapse STM during H_2 exposure at 2.5×10^{-7} Torr, showing the progressive decay of Al islands (I) and vacancy islands (V) due to H_2 dissociation and H spillover from Ti. (d–f) Similar image series for 2.3×10^{-5} Torr H_2. Outlines mark corresponding areas in different images.

To analyze the mechanism of the Ti-catalyzed H_2 dissociation, we performed DFT calculations on H_2 interacting with different configurations of Ti atoms near Al(111) (Figure 4 a). Transition states of H_2 dissociating to atomic H were

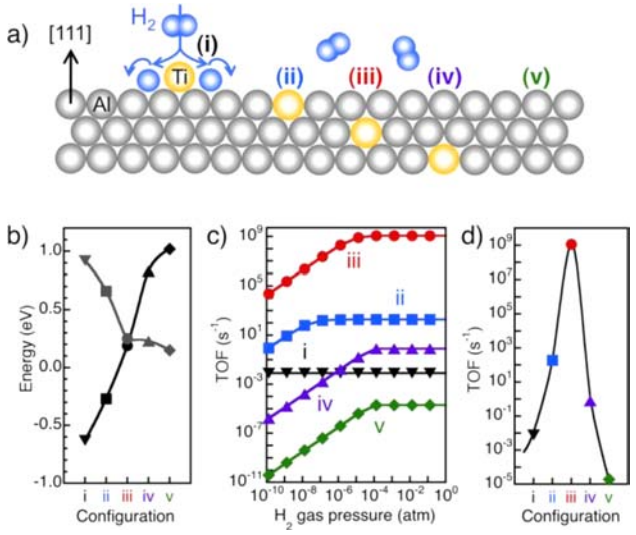

Figure 4. DFT-computed H_2 dissociation transition state energies and H spillover barriers and the resulting turnover frequencies (TOFs) for different placements of Ti near Al(111). (a) Schematic illustration of different configurations of Ti catalyst atoms near Al(111): (i) ad-Ti; (ii–iv) substitutional Ti in the (ii) surface layer, (iii) subsurface layer, and (iv) second subsurface layer of Al(111); and (v) Al(111) without Ti. (b) Site-dependent transition state energies for H_2 dissociation (black) and barriers for H spillover from the active site (gray). (c) TOFs per catalytic site for various H_2 pressures at 300 K for the Ti configurations shown in (a). (d) Maximum TOFs per catalytic site.

determined for (i) ad-Ti, (ii) surface Ti atoms in Al(111), (iii, iv) Ti-doped Al(111) surfaces capped by (iii) one or (iv) two atomic Al layers, and (v) pure Al(111) (for methods, see the SI); additionally, energy barriers for both H_2 dissociation (relative to the gas phase) and H transfer from the active site were computed (Figure 4 b). The H_2 dissociation barrier for Al(111) is very large (>1 eV; Figure 4 b and Figure S1); thus, a catalyst is needed to activate H_2 near room temperature, consistent with the need for Ti-doped Al* for Al hydrogenation and alane formation.[22−24] While the H_2 dissociation barriers for ad-Ti and substitutional surface Ti essentially vanish, the activation energies for H spillover from Ti to Al(111) are in both cases large (0.92 and 0.66 eV, respectively). A monolayer Al skin covering the Ti atoms has two effects (Figures S1 and S2). First, Al with subsurface Ti still provides a low activation energy for H_2 dissociation. Second, the barrier for spillover from the active site to Al(111) (0.23 eV) is nearly as low as the H diffusion barrier between threefold hollow sites on Al(111) (0.15 eV) and can be overcome at moderate temperatures. Burying Ti in deeper layers causes the barrier for H_2 dissociation to rise toward the high value on Al(111) (Figure S2). DFT-based kinetic Monte Carlo simulations confirmed substantial H trapping by surface Ti, which was absent for subsurface Ti (Figure S3 a). Thus, the H diffusivity on Al(111) with subsurface Ti is considerably higher than on mixed Al:Ti surfaces (Figure S3 b).

Figure 4 c shows the computed room-temperature turnover frequencies (TOFs) for the entire reaction (H_2 dissociation and H spillover) per catalytic site versus H_2 pressure for the different Ti configurations. The TOF for ad-Ti saturates at low H_2 pressure, consistent with poisoning of the catalytic sites by strongly bound H. The room-temperature residence time of H bound to a Ti adatom estimated from the TOF (Figure 4 d) exceeds 100 s. For surface Ti atoms in Al(111), the residence time is ~0.01 s, which is shorter than suggested by our STM observations (Figure 2 a). This may indicate that imaging is insensitive to the release of a H atom if it is rapidly replaced via another H_2 dissociation event. STM would then detect only the exchanges leading to occupancy of another binding site and may thus overestimate the residence time. Hence, we conclude that some H spillover from surface Ti/Al(111) is activated at room temperature, consistent with a recent report.[27] The H_2 pressure at which the computed TOF saturates increases as Ti is embedded in the Al matrix [(i) ad-Ti; (ii) surface Ti] and further as the Ti atoms are covered by an Al skin [(iii, iv) subsurface Ti; (v) pure Al]. The high saturation TOF required

dx.doi.org/10.1021/ja304203y | J. Am. Chem. Soc. 2012, 134, 10381−10384

in hydrogenation reactions is achieved only for Ti catalysts embedded in the Al surface and in the first subsurface layer (Figure 4 d). Subsurface Ti catalysts give by far the highest TOF, exceeding that of surface Ti by a factor of $\sim 6 \times 10^6$. The calculations predict that at our experimental H_2 pressures a significant population of atomic H on Al(111), detectable via Al(111) island/pit decay, should be generated only for subsurface Ti, in agreement with our experimental results

Our findings show that the overall activity of dilute Ti catalysts used to promote hydrogenation in Al-based hydrogen storage materials is governed by a competition between activation of H_2 dissociation and H spillover from the active site, both of which are strongly affected by the catalyst placement. Ti atoms placed in sites that provide the highest dissociation activity (ad-Ti; surface Ti) bind the products strongly and rapidly become poisoned, whereas a somewhat less active site (subsurface Ti) provides an optimal trade-off of moderate dissociation and spillover energies. The overall turnover frequency rises with increasing reactant pressure to a saturation level that is primarily limited by product spillover from the active site. These results are relevant in two contexts: heterogeneous catalysis with individual atoms as active sites and hydrogenation reactions involving Ti-doped Al. The existence of a catalyst site providing an optimal compromise between reactant activation and product spillover is likely a unifying theme among dilute alloy catalysts.[9] Controlling the catalyst placement during synthesis and calcination is clearly crucial, but a possible redistribution in-operando by diffusion or segregation, as determined by the reaction conditions (temperature, reactant composition and pressure),[28] also must be considered when designing and operating a dilute alloy catalyst. Ti-catalyzed Al hydrogenation is a case in point. We have identified a preferred placement of Ti catalysts in metallic Al that provides the highest rate of H production, but stabilizing this active configuration may be challenging. While vacuum annealing promotes Al-terminated surfaces by migration of Ti into subsurface layers,[19] an increase in the hydrogen chemical potential may reverse this trend and cause Ti surface segregation.[26] In addition to such segregation phenomena, selective Al removal during Al* hydrogenation can cause the redistribution and ultimately accumulation of Ti at or near the surface,[29] and this should also be considered in designing similar systems for optimum hydrogenation rates.

■ ASSOCIATED CONTENT

Ⓢ Supporting Information

Experimental and computational methods, calculation of TOFs, kinetic Monte Carlo calculations of H diffusion on Al(111) and Al(111):Ti, and Figures S1−S3. This material is available free of charge via the Internet at http://pubs.acs.org.

■ AUTHOR INFORMATION

Corresponding Author

psutter@bnl.gov

Notes

The authors declare no competing financial interest.

■ ACKNOWLEDGMENTS

This work was supported by the Materials Sciences Division of the Office of Basic Energy Sciences, U.S. Department of Energy (DOE-BES) under FWP BO-130. Research carried out at the Center for Functional Nanomaterials and the Chemistry Department at Brookhaven National Laboratory was supported by DOE-BES under Contract DE-AC02-98CH10886.

■ REFERENCES

(1) Rodriguez, J. A. *Surf. Sci. Rep.* **1996**, *24*, 223.
(2) Jiang, X.; Gur, T. M.; Prinz, F. B.; Bent, S. F. *Chem. Mater.* **2010**, *22*, 3024.
(3) Greeley, J.; Mavrikakis, M. *Catal. Today* **2006**, *111*, 52.
(4) Hammer, B.; Nørskov, J. K. *Adv. Catal.* **2000**, *45*, 71.
(5) Greeley, J.; Nørskov, J. K.; Mavrikakis, M. *Annu. Rev. Phys. Chem.* **2002**, *53*, 319.
(6) Zhang, J.; Vukmirovic, M. B.; Xu, Y.; Mavrikakis, M.; Adzic, R. R. *Angew. Chem., Int. Ed.* **2005**, *44*, 2132.
(7) Jacobsen, C. J. H.; Dahl, S.; Clausen, B. S.; Bahn, S.; Logadottir, A.; Nørskov, J. K. *J. Am. Chem. Soc.* **2001**, *123*, 8404.
(8) Hammer, B.; Nørskov, J. K. *Surf. Sci.* **1995**, *343*, 211.
(9) Kyriakou, G.; Boucher, M. B.; Jewell, A. D.; Lewis, E. A.; Lawton, T. J.; Baber, A. E.; Tierney, H. L.; Flytzani-Stephanopoulos, M.; Sykes, E. C. H. *Science* **2012**, *335*, 1209.
(10) Baber, A. E.; Tierney, H. L.; Lawton, T. J.; Sykes, E. C. H. *ChemCatChem* **2011**, *3*, 607.
(11) Schlapbach, L.; Zuttel, A. *Nature* **2001**, *414*, 353.
(12) Graetz, J. *Chem. Soc. Rev.* **2009**, *38*, 73.
(13) Bogdanovic, B.; Schwickardi, M. *J. Alloys Compd.* **1997**, *253*−*254*, 1.
(14) Sakaki, K.; Nakamura, Y.; Akiba, E.; Kuba, M. T.; Jensen, C. M. *J. Phys. Chem. C* **2010**, *114*, 6869.
(15) Peles, A.; Van de Walle, C. G. *Phys. Rev. B* **2007**, *76*, No. 214101.
(16) Wilson-Short, G. B.; Janotti, A.; Hoang, K.; Peles, A.; Van de Walle, C. G. *Phys. Rev. B* **2009**, *80*, No. 224102.
(17) Felderhoff, M.; Klementiev, K.; Grunert, W.; Spliethoff, B.; Tesche, B.; Bellosta von Colbe, J. M.; Bogdanovic, B.; Hartel, M.; Pommerin, A.; Schuth, F.; Weidenthaler, C. *Phys. Chem. Chem. Phys.* **2004**, *6*, 17.
(18) Graetz, J.; Reilly, J. J.; Johnson, J.; Ignatov, A. Y.; Tyson, T. A. *Appl. Phys. Lett.* **2004**, *85*, 500.
(19) Muller, E.; Sutter, E.; Zahl, P.; Ciobanu, C. V.; Sutter, P. *Appl. Phys. Lett.* **2007**, *90*, No. 151917.
(20) Bellosta von Colbe, J. M.; Schmidt, W.; Felderhoff, M.; Bogdanovic, B.; Schuth, F. *Angew. Chem., Int. Ed.* **2006**, *45*, 3663.
(21) Chaudhuri, S.; Muckerman, J. T. *J. Phys. Chem. B* **2005**, *109*, 6952.
(22) Lacina, D.; Reilly, J.; Celebi, Y.; Wegrzyn, J.; Johnson, J.; Graetz, J. *J. Phys. Chem. C* **2011**, *115*, 3789.
(23) Lacina, D.; Wegrzyn, J.; Reilly, J.; Celebi, Y.; Graetz, J. *Energy Environ. Sci.* **2010**, *3*, 1099.
(24) Graetz, J.; Wegrzyn, J.; Reilly, J. J. *J. Am. Chem. Soc.* **2008**, *130*, 17790.
(25) Ratke, L.; Voorhees, P. W. *Growth and Coarsening: Ostwald Ripening in Material Processing*; Springer: Berlin, 2002.
(26) Stumpf, R.; Bastasz, R.; Whaley, J. A.; Ellis, W. P. *Phys. Rev. B* **2008**, *77*, No. 235413.
(27) Chopra, I. S.; Chaudhuri, S.; Veyan, J. F.; Chabal, Y. J. *Nat. Mater.* **2011**, *10*, 884.
(28) Tao, F.; Grass, M. E.; Zhang, Y.; Butcher, D. R.; Renzas, J. R.; Liu, Z.; Chung, J. Y.; Mun, B. S.; Salmeron, M.; Somorjai, G. A. *Science* **2008**, *322*, 932.
(29) Graham, D. D.; Graetz, J.; Reilly, J.; Wegrzyn, J. E.; Robertson, I. M. *J. Phys. Chem. C* **2010**, *114*, 15207.